



Research Repository UCD

Title	Calculation of the Dynamic Allowance for Railway Bridges from Direct Measurement
Authors(s)	Connolly, L. C., Hajializadeh, Donya, Leahy, Cathal, O'Connor, Alan, O'Brien, Eugene J., Bowe, Cathal
Publication date	2016-04-08
Publication information	Connolly, L. C., Donya Hajializadeh, Cathal Leahy, Alan O'Connor, Eugene J. O'Brien, and Cathal Bowe. "Calculation of the Dynamic Allowance for Railway Bridges from Direct Measurement." Civil-Comp Press, 2016.
Conference details	Railways 2016: The Third International Conference on Railway Technology: Research, Development and Maintenance, Sardinia, Italy, 5-8 April 2016
Publisher	Civil-Comp Press
Item record/more information	http://hdl.handle.net/10197/9243
Publisher's version (DOI)	10.4203/ccp.110.138

Downloaded 2024-04-18 15:22:20

The UCD community has made this article openly available. Please share how this access benefits you. Your story matters! (@ucd_oa)



© Some rights reserved. For more information

Calculation of the Dynamic Allowance for Railway Bridges from Direct Measurement

*L.C. Connolly, E.J. O'Brien, A.J. O'Connor, E.J. Bowe, C. Leahy, D. Hajialiazadeh,
I. Roughtan O'Donovan Innovative Solutions, Consulting Engineers*

Abstract

In a traditional deterministic assessment, a dynamic amplification factor (DAF) is applied to the static loading in order to account for dynamics. The codified DAF values are appropriately conservative in order to consider the wide range of structures and load effects to which they are applied. In the current analysis, a site specific assessment dynamic ratio (ADR) is calculated from direct measurement on an 80 year old steel truss Railway Bridge. The ADR is defined as the ratio of characteristic total stress to the characteristic static stress. The application of ADR is a relatively new concept which has rarely been considered for railway bridges. An assessment performed on the bridge in question showed a decrease in the dynamic allowance when considering the site specific ADR, corresponding to a 26% decrease in calculated stress. The measurements available were also used to derive a robust stochastic model for dynamic allowance which considered the correlation between DAF and stress level. The developed model was applied to a probabilistic assessment and resulted in a 9% increase in reliability.

Keywords: dynamics, DAF, ADR, truss, bridge, probabilistic, assessment, reliability, monitoring, vibration, signal, filter.

1 Introduction

In order to account for dynamics in bridge design and assessment, a Dynamic Amplification Factor (DAF) is typically applied to static loading. This is defined as the total (static + dynamic) load effect, LE_{Total} , to the static load effect, LE_{Static} , for a particular event.

$$DAF = \frac{LE_{Total}}{LE_{Static}} \quad (1)$$

It has been shown that in many cases the factors employed have been over-conservative [1]. This is considered to be acceptable for bridge design codes in order to consider the wide range of structures and load effects to which they are applied. However, for existing structures, this conservatism can result in costly and unnecessary repairs being put in place. Previous research has shown that the DAFs defined in most codes are appropriate for lower levels of loading, such as single event crossings with light trucks on road bridges [1]. However, for heavier loads, measured DAFs have been shown to be significantly lower [1]. One possible reason for this is the speed reduction associated with heavy vehicles, which reduces

dynamic amplification as noted by Frýba [2]. The formulation of DAF in Equation 1 also fails to account for the probability of maximum static and total load effects occurring for separate events. The Danish roads directorate (DRD) document on reliability based classification of the load carrying capacity of existing road bridges [3], suggests the use of a stochastic increment for dynamic amplification for gross vehicle weight (GVW) modelled as a normally distributed variable with mean and standard deviation equal to $41.5/\text{GVW}$, where the GVW is in kN. The result of this model is that dynamics reduce with increasing vehicle weight, as shown in Figure 1.

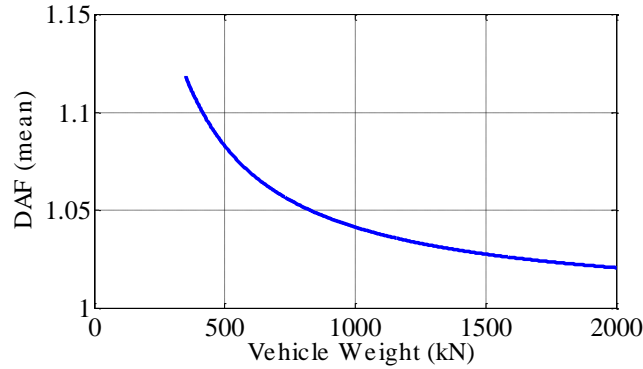


Figure 1. Mean DAF versus vehicle weight from Danish Roads Directorate [3]

In order to alleviate the drawbacks associated with traditional codified DAFs, various authors [1,4,5] have introduced the concept of an Assessment Dynamic Ratio (ADR), defined as the ratio of the characteristic total (static + dynamic) load effect, $\tilde{L}E_{Total}$, to the characteristic static load effect, $\tilde{L}E_{Static}$.

$$ADR = \frac{\tilde{L}E_{Total}}{\tilde{L}E_{Static}} \quad (2)$$

1.1 Calculation of ADR

In order to evaluate the ADR for a specific bridge, the characteristic total and characteristic static load effects are required. OBrien et al [4] used the output from a Bridge Weigh-in-Motion (WIM) system to obtain the strain signals associated with total (static + dynamic) strain. Characteristic static strains were calculated by statistical extrapolation. The WIM system used also calculates a ‘measured’ static influence line for the structure. This was used in conjunction with the measured axle weights to infer the strains associated with the static response. The characteristic total and static strains were then used to calculate the ADR. A disadvantage in the procedure used by OBrien et al [4] is that the inaccuracies associated with calculation of axle weights using bridge WIM result in the introduction of a bias in the calculation of ADR. A similar procedure is used in SAMARIS [1]. In each case, an additional disadvantage is the requirement of cumbersome calibration of the Bridge WIM system, which is not required for the approach adopted in this paper.

Simulation can also be used to calculate characteristic load effects for both static and dynamic response. The research performed as part of SAMARIS [1]

demonstrated this. Once again, the conclusion was drawn that the dynamic amplification reduces as the magnitude of the load effect increases. Despite the advantages associated with site-specific ADR calculation, the theory has rarely been applied to railway bridges. One possible reason for this is the lack of variation in the distribution of trains that pass over a specific bridge, making it difficult to perform meaningful statistical extrapolations. The procedure was first introduced by Cantero [5], where it was concluded that a smaller recommended allowance for dynamics can be safely accommodated for various bridge configurations. Cantero [5] calculated characteristic load effects by performing Monte Carlo simulation on a train-track-bridge interaction model, accounting for track irregularities. The bridge model considered was a 2-dimensional Euler-Bernoulli beam. Considering the number of inputs and the large amount of computing power required for this type of simulation, it may be difficult to perform the analysis on a more complex 3-dimensional bridge model. Therefore, a different approach is proposed in this paper.

A case study bridge (see Section 3.1) is used to calculate a site-specific ADR, incorporating a structural health monitoring (SHM) system. Strain signals from the bridge, encompassing total (static + dynamic) strain, are filtered using band-pass filtering algorithms to remove dynamics. Maximum daily strains are then used to extrapolate characteristic total and static strains. The site specific ADR is then calculated for a critical member. The implications of the calculation are then demonstrated in terms of both a deterministic and probabilistic assessment.

2 Demonstration of concept – filtering of dynamics

In order to demonstrate and validate the methodology employed to filter the dynamic response, consider a simply supported beam of length ‘L’, subjected to a moving point load ‘P’, moving at a speed ‘c’ shown in Figure 2.

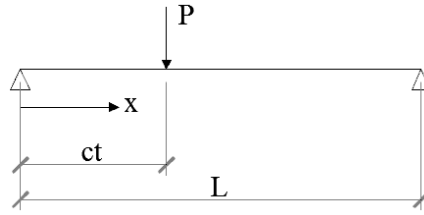


Figure 2. Simply supported beam subjected to a moving point load

The dynamic displacement response of the beam was formulated by Frýba [2]:

$$v(x, t) = v_0 \sum_{j=1}^{\infty} \frac{1}{j^2[j^2(j^2 - \alpha^2)^2 + 4\alpha^2\beta^2]} \left[j^2(j^2 - \alpha^2) \sin j\omega t - \frac{j\alpha[j^2(j^2 - \alpha^2) - 2\beta^2]}{(j^4 - \beta^4)^{1/2}} e^{\omega_b t} \sin \omega'_{(j)} t - 2j\alpha\beta(\cos j\omega t - e^{-\omega_b t} \cos \omega'_{(j)} t) \right] \sin \frac{j\pi x}{L} \quad (3)$$

where

$$\alpha = \frac{cl}{\pi} \left(\frac{\mu}{EJ} \right)^{1/2} \quad (4)$$

$$\beta = \frac{\omega_b l^2}{\pi^2} \left(\frac{\mu}{EJ} \right)^{1/2} \quad (5)$$

and,

x = length coordinate with origin at the left hand end of the beam,

t = time since the force arrived on the beam,

$v(x, t)$ = vertical displacement at point x and time t ,

j = mode of vibration,

ω = circular frequency of damping of the beam,

E = Young's modulus of the beam,

J = constant moment of inertia of the beam cross section,

μ = constant mass per unit length of the beam

The result is calculated for a 20 m span concrete beam with a breadth of 1 m and a depth of 0.8 m. A 200 kN point load is considered with a velocity of 20 m/s. By computing the first derivative of Equation 3 with respect to x , the dynamic strain response can be derived for the beam due to the moving load. Figure 3 illustrates the total (dynamic + static) strain in comparison to the static response. For this example, the dynamic increment may be considered as the ratio between the maximum total (dynamic + static) and maximum static strain, which corresponds to a value of 1.14. A total of 50 modes of vibration are considered in Figure 3, although the result is approximately the same for around 10 modes, indicating that the majority of vibration is associated with the first few modes. By computing the second derivative of Equation 3 with respect to time, the acceleration response of the beam can be obtained. A Fourier transform can then be applied to the acceleration signal to obtain the natural frequencies of the beam. These can be compared to the theoretic natural frequencies of a simply supported beam (Figure 4). The j^{th} natural frequency of this beam, as formulated by Frýba [2], is calculated as:

$$\alpha = \frac{j^2 \pi}{2L^2} \left(\frac{EJ}{\mu} \right)^{1/2} \quad (6)$$

Figure 4 illustrates the first 5 natural frequencies of the beam, computed by a Fast Fourier Transform (FFT) compared to the theoretical frequencies. It is clear that for the system in question, the beam does not vibrate at its second or fourth frequency.

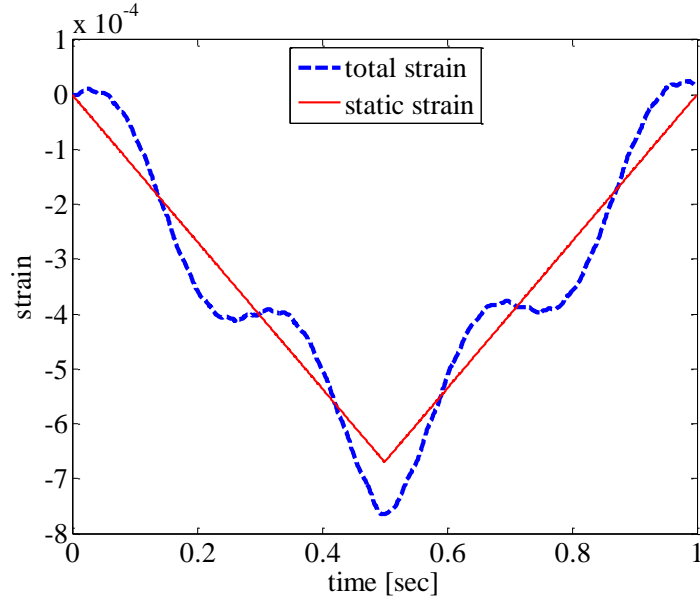


Figure 3. Total (static + dynamic) and static strain response of theoretical concrete beam

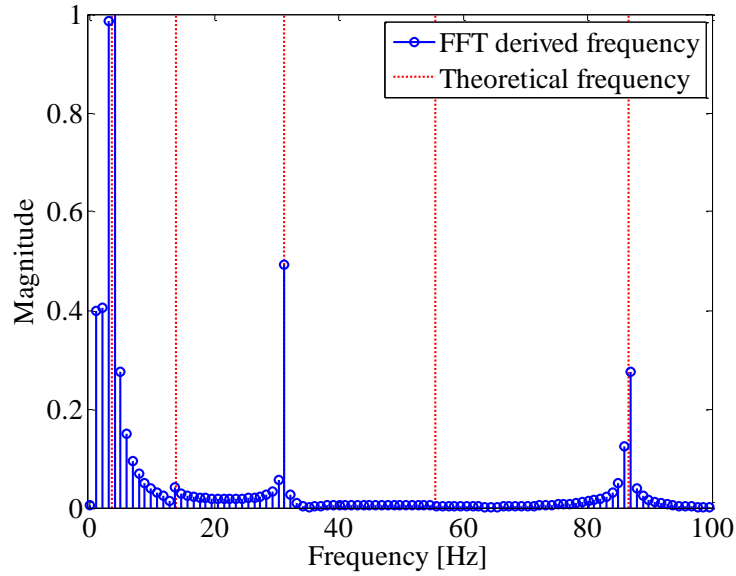


Figure 4. Theoretical and FFT computed natural frequencies of concrete beam

In practice, the dynamic strain is measured by the sensor on the bridge. As stated above, in order to calculate the ADR, both the static and dynamic response is required. The static response is obtained by applying a filter to the total (dynamic + static) response. Digital filters are often employed to remove specific frequency domains from an input signal [6]. This is achieved by passing an input signal through a transfer function, or filter signal. A low-pass filter is one which attenuates the parts of the input signal which relate to frequencies above a certain value,

referred to as the “cut-off” of the filter [6]. In this section, it will be shown that the concept is well suited to the removal of dynamics from measured strain signals. This is because the portion of the total (dynamic + static) strain signal which relate to dynamic vibration can be removed by applying a low pass filter. The remaining portion of the signal, which relates to static strain, will not be affected. A low-pass Butterworth signal filter was designed for this purpose. The Butterworth filter was chosen as it has low ripple in the pass band and stop band, meaning that the static response is not altered. Of course, a critical input to the filter is the first natural frequency, as this defines the cut-off. Vibration associated with higher frequencies will also be filtered out of the total (dynamic + static) response, although their affect on the dynamic response is expected to be low.

As Butterworth signal filters have a slower roll-off than, for example, Chebyshev signal filters [6,7], the cut-off was set at a value 10% below the first natural frequency of the beam, to ensure that all vibration associated with the first natural frequency was removed. Figure 5 shows the result of passing the total strain signal from Figure 3 through a 7th order low-pass Butterworth filter. It is clear from Figure 5 that the majority of the dynamic oscillation was removed from the total strain signal, (i.e. the ratio of the maximum static strain to the maximum filtered total strain is 1.00). In the following section, the theory will be applied to a case-study bridge to calculate a site-specific dynamic allowance.

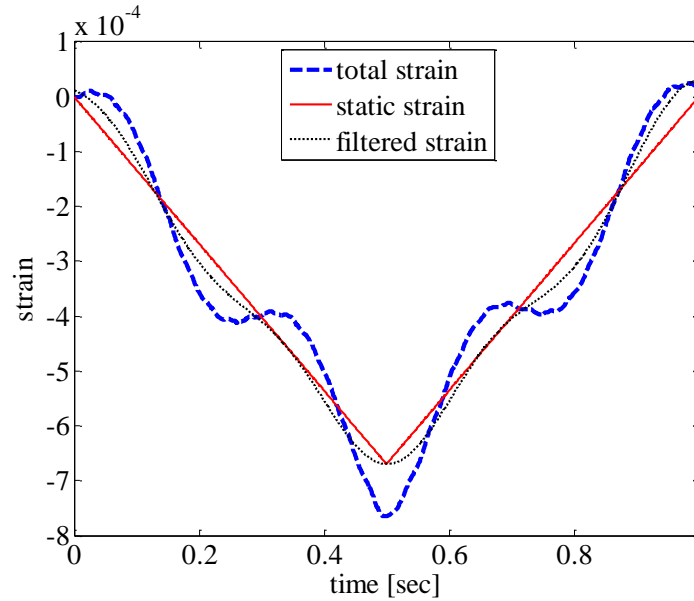


Figure 5. Filtering of total (static + dynamic) strain response for theoretical beam

3 Calculation of site-specific ADR for the Boyne Viaduct

3.1 Assessment

The Boyne Viaduct (Figure 6) in Drogheda, Co. Louth, Ireland, is around 80 years old and consists of three steel spans of 40, 80 and 40 metres. Only the central span was considered for this study. The riveted steel truss structure has an arched profile consisting of 10 bays with cross beams spanning between the node points of the

truss. The ballasted track is supported on a steel deck plate over the rail bearers, which span between the cross beams.



Figure 6: Central span of the Boyne Viaduct, Drogheda, Co. Louth, Ireland.

An FE model was developed and is illustrated in Figure 7. The model was used to perform a deterministic assessment of the structure in accordance with the design manual for roads and bridges (DMRB, [8,9]). A full description of the assessment can be found in Connolly et al. [10]. The assessment showed that the critical rail bearers of the structure were the only elements to fail the assessment. The load effect in question was ULS yielding and the overstress was 6%.

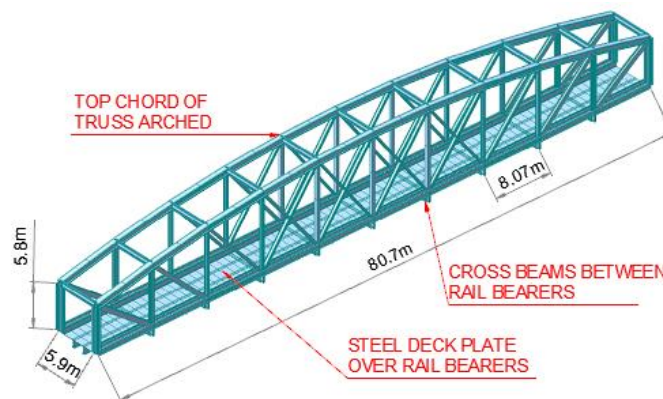


Figure 7. finite element (FE) model of the Boyne Viaduct central span [11]

After having failed the deterministic assessment, the rail bearers of the structure were assessed probabilistically under ULS yielding. The majority of the stochastic modelling was performed in accordance with the guidelines of the Danish Roads Directorate [3]. Full details of the probabilistic assessment can be found in [10]. FORM analysis [12] was used to compute the reliability index, β , for the rail bearer. The analysis converged to a value of $\beta = 3.4$. The target level of reliability may be specified by the client, but ISO 2394:1998 [13] recommends a value of 3.8 for a “moderate” cost of safety measures and a “great” consequence of failure. The

corresponding level recommended by the Joint Committee on Structural Safety is 4.4 [14]. In either case, the element in question may be said to have failed the probabilistic assessment.

Within the deterministic assessment, the dynamic allowance was calculated from the guidelines in the DMRB [8]. A value of 1.42 was calculated. As stated in Section 1, this DAF may be inappropriately conservative for the structure in question. For the probabilistic assessment, the DAF was modelled in a manner similar to the DRD guidelines [3] as follows:

$$DAF = 1 + \varepsilon \quad (7)$$

The dynamic increment (ε) was modelled as a normally distributed variable with a Coefficient of Variation (CoV) of 1.0 as recommended in the DRD [3]. However, the mean value specified in the DRD guidelines [3] relate to road bridges. Therefore, the mean value was determined as that which resulted in a 98% fractile value equal to the deterministic increment (0.42), in line with work by O'Connor et al. [15]. This resulted in a normally distributed variable for the ε increment with mean and standard deviation equal to 0.14. It is clear that the stochastic modelling of dynamic allowance considered here was based on codified loading, and does not take account of the inverse relationship between vehicle weight and DAF, as noted in [1].

The assessment performed was used to define an instrumentation strategy for the structure. Four rosette strain gauges were placed on the bottom flanges of the critical rail bearers and the most critical cross beam. In addition to the work performed in this paper, these gauges will be used for model validation and fatigue analysis. The bottom chord of the truss was instrumented with triaxial accelerometers. Figure 8 shows the strain gauges and accelerometers installed on the structure.

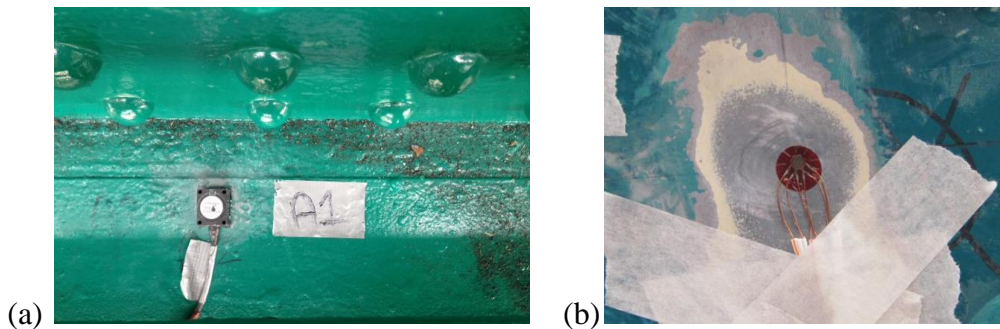


Figure 8. Accelerometer (a) and strain gauge (b) on the Boyne Viaduct

3.2 Evaluation of natural frequencies

In order to identify the optimum locations for the accelerometers on the Boyne viaduct, a modal analysis was carried out on the FE model. Elevations of the first two mode shapes of the structure are illustrated In Figure 10. Their respective frequencies of vibration were calculated as 3.9 and 9.2 Hz. Based on the mode shapes, accelerometers were placed at centre span and at one third span.

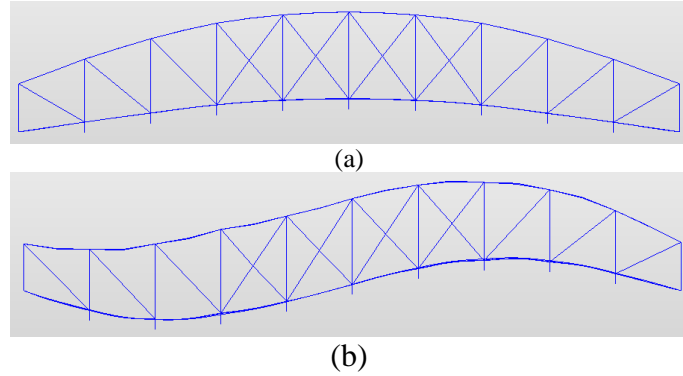


Figure 9. First (a) and second (b) vertical mode shapes of the Boyne Viaduct

Vibration responses from the accelerometers at the central span and one third span are illustrated in Figure 10.

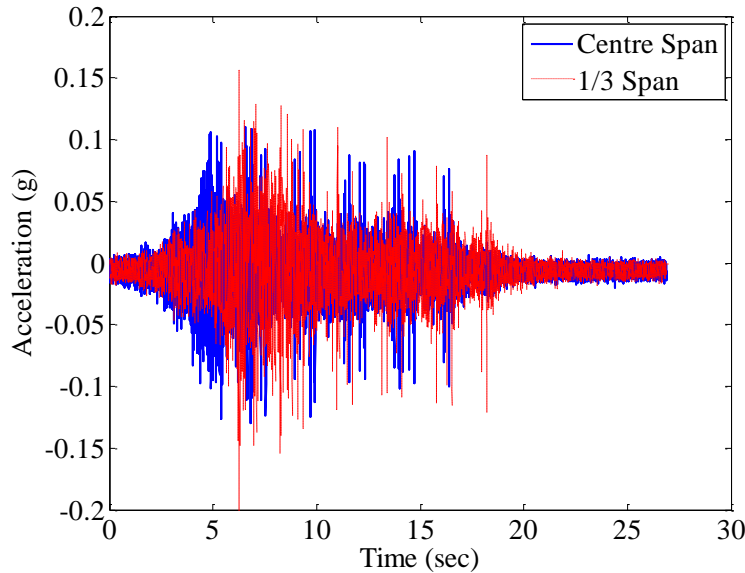


Figure 10. Vertical acceleration at centre span (a) and one third span (b) of the Boyne Viaduct

As stated in Section 2 above, a critical input to the low-pass filter is the natural frequency of vibration of the structure. FFTs were calculated for each of the acceleration responses at centre span and one third span and are illustrated in Figure 11. It should be noted that the Fourier Transforms shown in Figure 11 are based on all signals (from all events) together. It is clear that for both FFTs, there is a peak around 10Hz. Most of the FFTs for each individual event also showed a peak at this frequency. Therefore, this was the cut-off defined for the low-pass filter. Each FFT also showed a sharp peak at approximately zero, but this was attributed to signal noise and was ignored.

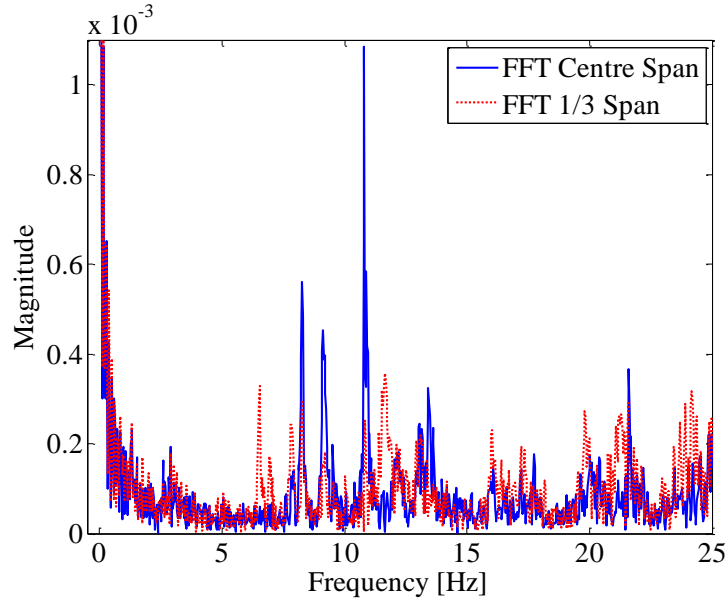


Figure 11. FFT of vertical acceleration at centre span (a) and one third span (b) of the Boyne Viaduct

3.3 Removal of dynamics

In order to remove the dynamics from the total (static + dynamic) portion of the strain signals for the centre of the rail bearer, the low-pass filter discussed in Section 2 was applied to the strain signals. It was found that various levels of dynamic amplification were noted for different events. Figure 12 shows an example with a maximum DAF (per train) of 1.07, while Figure 13 shows an example with a maximum DAF (per train) of 1.02. It should be noted that the strain signals shown are principal strains for the element in question, which are considered to be appropriate for the critical yield criterion in the assessment. The figures also show a magnified view of selected peaks.

It is clear from Figures 12 and 13 that the DAF considered in the DMRB is conservative for the bridge in question as the maximum DAF detected in the monitoring period is 24% below the DAF calculated as recommended in the DMRB [8]. This is expected, considering that the age of the structure may indicate that it is over-designed. In addition, the ballasted track may tend to reduce dynamic amplification for the rail bearers, as noted in the Eurocode [16]. The authors also note that there is a speed restriction on the bridge of 50 km/hr, which will also result in low levels of dynamic amplification as noted by Frýba [2].

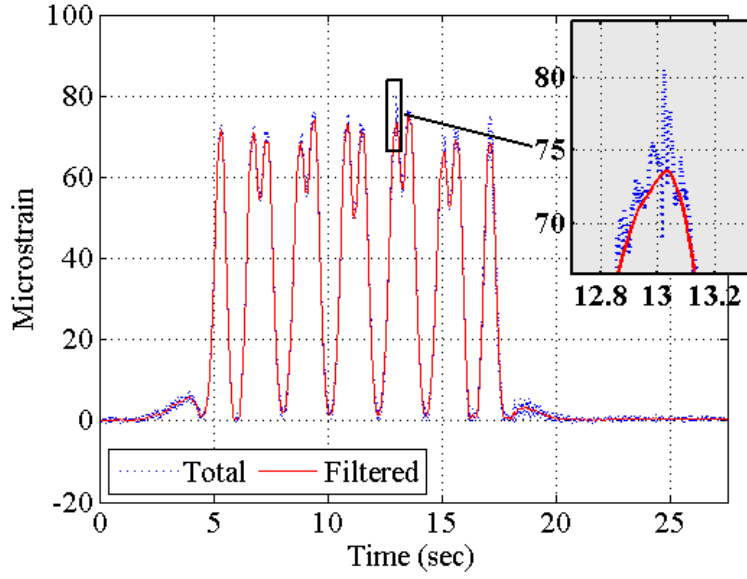


Figure 12. Low-pass filter applied to strain data at centre of rail bearer – DAF = 1.07

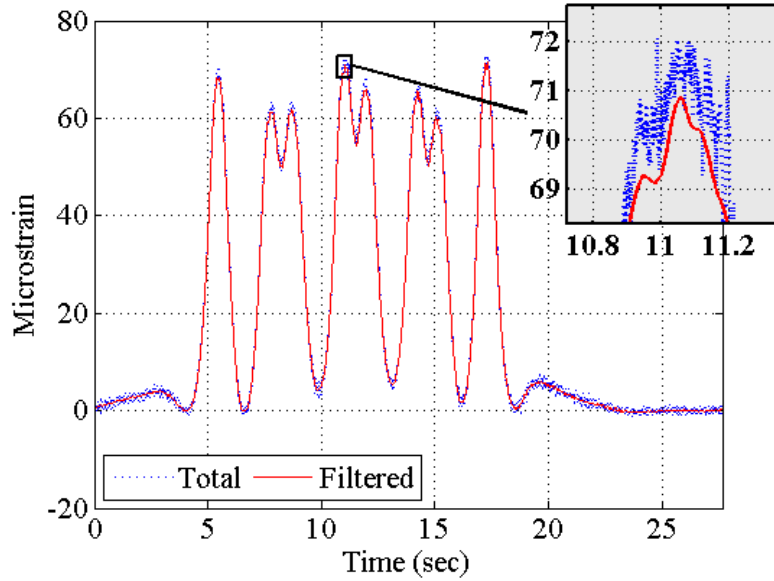


Figure 13. Low-pass filter applied to strain data at centre of rail bearer – DAF = 1.02

3.4 Calculation of dynamic allowance.

3.4.1 Assessment Dynamic Ratio (ADR)

In order to evaluate the characteristic ADR from Equation 2, the characteristic total (static + dynamic) load effect, $\bar{L}E_{Total}$, and the characteristic static load effect, $\bar{L}E_{Static}$, are required. In order to derive characteristic load effects, a Generalised Extreme Value (GEV) distribution is fitted to the maximum daily strains by maximum likelihood estimation. 20 days of measurement was available at the time

of submission, consisting of around 340 train passing events. The characteristic load effect is calculated at the appropriate return period. A return period of 1000 years is taken in the Eurocode for design [16]. A 75-year return period is considered here for an existing bridge. Figure 14 is plotted on probability paper. The 75 year return period for maximum daily values (250 weekdays in a year) is given as:

$$-\ln(-\ln(1 - 1/[75 * 250])) \approx 9.84 \quad (7)$$

In Figure 14 the dashed line represents the GEV fit to the static strain, while the solid line represents the GEV fit to the total (static + dynamic) strain.

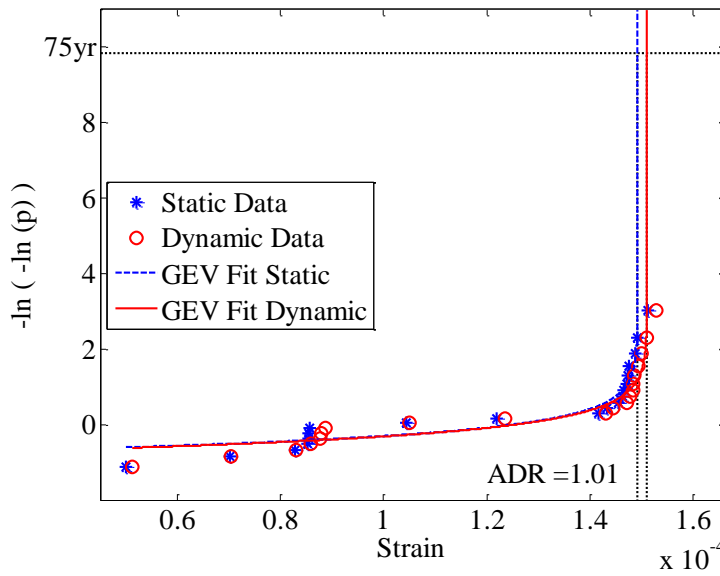


Figure 14. Extrapolation of total and static strain for ADR

The concave upward shape of the graph in Figure 14 indicates Weibull behaviour [12]. The ADR is calculated as 1.012. However, in order to allow a margin for error, an ADR of 1.05 is suggested for this member. This is considered for deterministic assessment in Section 4.

3.4.2 DAF distribution

For the probabilistic assessment, a distribution of DAF is required. For this purpose, a histogram of all DAFs (for individual events) is plotted in Figure 15. Normal and Lognormal distributions are fitted to the data. DAF is usually modelled as a normally distributed variable [3]. However, it is clear from the figure that the lognormal distribution is more appropriate for the data. This was confirmed with a goodness of fit test.

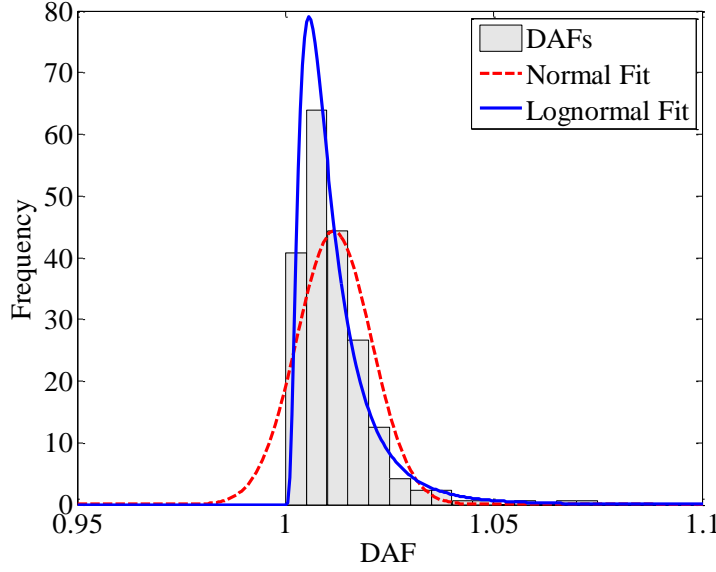


Figure 15. Fit of lognormal distribution to dynamic amplification

It should be noted that the distributions were fitted to the dynamic increment, ε , and not the DAF. The lognormal parameters of the dynamic increment, ε , of μ_{\log} and σ_{\log} are -4.69 and 0.71, respectively. This corresponds to an associated normal mean and standard deviation of 0.012 and 0.01, respectively. Convolution is then used to obtain the maximum yearly distribution of DAF:

$$F(x) = f(x)^N \quad (8)$$

Where $F(x)$ is the maximum yearly distribution, $f(x)$ is the daily distribution, and:

$$N = [\text{no. trains per day}] \times [\text{no. working days}] = 16 \times 250 = 4000 \quad (9)$$

Therefore, the yearly distribution for the dynamic increment, ε , considered appropriate for probabilistic assessment can be calculated and is given by a lognormal distribution with parameters μ_{\log} and σ_{\log} equal to -2.12 and 0.23. This corresponds to an associated normal mean and standard deviation of 0.12 and 0.03, respectively. It is clear that this is less conservative than the previous distribution employed for DAF. It may also be concluded here that the assumption of the DRD guidelines [3] that the coefficient of variation in DAF is equal to 1.0 may not be appropriate for railway structures.

3.4.3 Stress varying DAF distribution

The distribution derived for DAF in Section 3.4.2 is calculated for the specific bridge element in question. However, consideration is not given to the trend of high DAFs corresponding to lower stresses [1]. For this reason, a stress varying lognormal distribution is fit to the DAFs of Figure 15. The principal stress is calculated from Equation 10. In Equation 10, E and ν are the Young's modulus and

Poisson's ratio of steel, respectively. The ε values correspond to the strains on each of the three gauges of the stacked rectangular rosette used.

$$\frac{E}{2} \left(\frac{\varepsilon_1 + \varepsilon_3}{1 - \nu} \pm \frac{1}{1 + \nu} \sqrt{(\varepsilon_1 - \varepsilon_2)^2 + (\varepsilon_2 - \varepsilon_3)^2} \right) \quad (10)$$

Figure 16 illustrates a contour plot of the stress-varying lognormal fit to the distribution of the dynamic increment for each event. The parameters of the distribution (μ_{\log} and σ_{\log}) vary with stress according to linear trends. The stress-varying distribution is fitted to the measured data using maximum likelihood estimation which determines the parameters of the linear trends. It can be seen that the approach is effective for modelling the reduction in DAF with increase in stress. The approach is similar to that used by OBrien et al. [17] who used a time-varying distribution of traffic loading to model growth in traffic loading over time. It is important to understand that this is not a three dimensional statistical distribution but rather a two dimensional distribution that changes with stress.

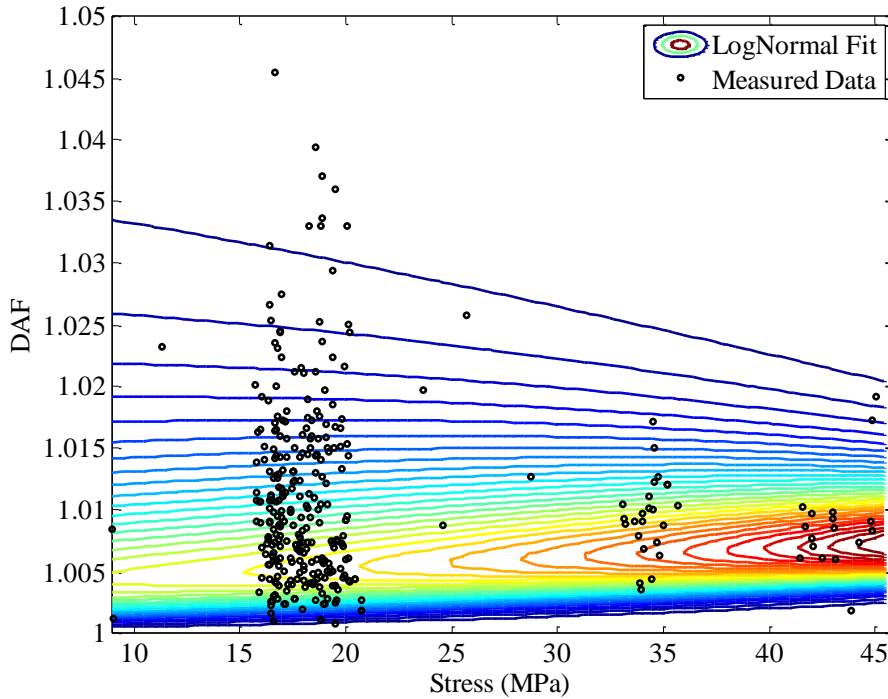


Figure 16. Stress varying lognormal distribution for DAF

It is clear in Figure 16 that the inverse relationship between stress and DAF is not as pronounced as was found in the literature [1]. This may be due to the low levels of dynamic vibration on the Structure and also due to the limited data available. Convolution was again used, as in Section 3.4.2, in order to derive the maximum yearly distribution. A 3D view of the yearly distribution is shown in Figure 17. It is clear that the standard deviation reduces as the stresses increase.

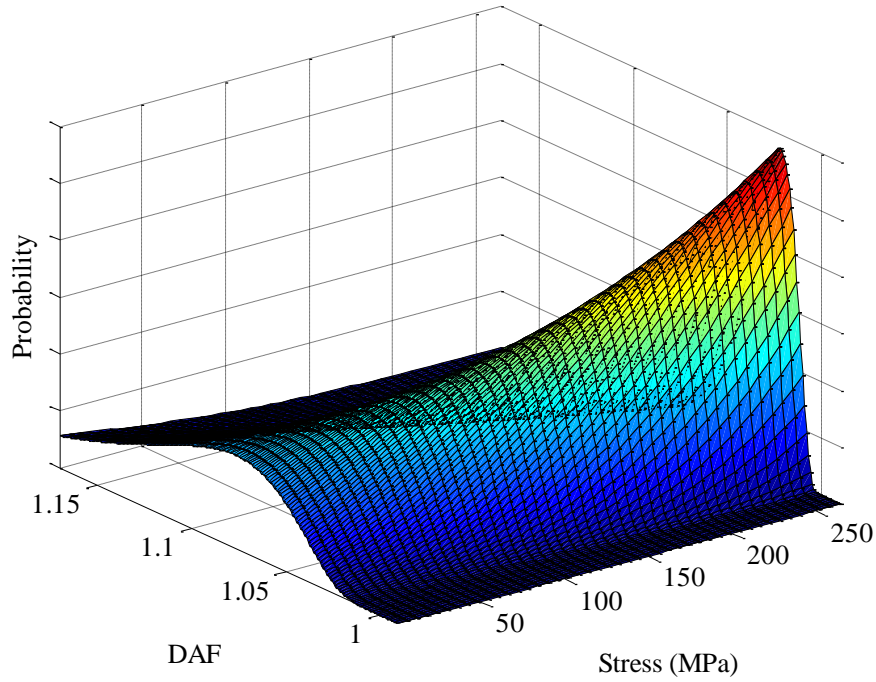


Figure 17. 3D view of maximum yearly stress varying lognormal distribution for DAF

4 Implications for safety assessment

The ADR calculated in Section 3.4.1 is considered applicable to the deterministic assessment. The value of 1.05 calculated is 26% below the value of 1.42 determined from the procedure outlined in the DMRB [8]. This results in the 6% overstress previously noted being reduced to a 20% under stress. It is clear that this could alleviate the need for further assessment.

The probabilistic analysis has been reconsidered with application of the more appropriate lognormal distribution for DAF, as determined in Section 3.4.2. The use of this distribution has been shown to result in an increase in the β -value from 3.4 to 3.5. As discussed in Section 3 above, this may still be considered to be insufficient for ULS failure under the guidelines of the JCSS [14]. Therefore, it is considered appropriate to consider the stress dependant distribution derived in Section 3.4.3.

In the probabilistic assessment, all parameters which relate to the load and resistance Equation of the ULS were modelled stochastically. This means that the static analysis was run 100,000 times, varying each parameter by randomly sampling from a distribution with a mean value (μ), and standard deviation (σ). A Matlab random number generator was used to perform the sampling. The stress varying distribution derived in Section 3.4.3 allowed sampling from a separate distribution for DAF, depending on the stress level. This procedure resulted in a further increase in the β -value to 3.7.

5 Conclusions and recommendations

A deterministic and subsequent probabilistic assessment was carried out on an 80 year old riveted steel truss railway bridge. The bridge was shown to have an insufficient level of reliability under ULS yielding. Data from instrumentation on the bridge was used to derive a more appropriate dynamic allowance. The assessments were then re-formulated with consideration of the new representation of dynamic allowance.

The traditional DAF defined in the DMRB was replaced with the Assessment Dynamic Ratio (ADR). The application of ADR resulted in a reduction in the utilisation for the critical element and limit state from 6% over-stress to 20% under-stress. Therefore, the procedure developed could have shown the bridge to have sufficient capacity prior to the undertaking of a probabilistic assessment.

A stochastic distribution was derived for the maximum yearly dynamic increment from the distribution of DAFs for individual events. This was shown to result in a 3% increase in reliability index, β , than that which was originally calculated. A stress varying distribution was also derived for DAF and this was also considered in the probabilistic assessment. This was shown to result in an increase in reliability of 9% from the original calculation.

The procedure developed herein is considered to have significant advantages over previous methods developed in the literature. For example, the expensive installation of WIM systems (and associated error) is alleviated. In addition, the development of complex and intensive dynamic interaction FE models is not required. Indeed, the procedures developed herein may be applied as an afterthought to any structure with a sufficient Structural Health Monitoring System installed.

It is considered that subsequent data to the 20-day period used in this analysis would be beneficial to provide a better representation of the stochastic distribution. Therefore, it is recommended that the models developed be re-calculated after a longer monitoring period has elapsed. It would also be beneficial to apply the method to another structure with higher levels of dynamic amplification in order to consider a wider range for the stress varying DAF distribution.

Acknowledgements

The research leading to these results was part of the DESTination RAIL project, a project funded by the EU Horizon 2020 Programme under call H2020-MG-2014 Mobility for Growth. Grant agreement no: 636285. The authors also gratefully acknowledge Iarnród Éireann, for facilitating the research associated with the Boyne Viaduct.

References

- [1] SAMARIS report D30, “Guidance for the Optimal Assessment of Highway Structures”, ZAG Ljubljana, <http://samaris.zag.si/>, 2006.
- [2] Fryba, L., “Vibration of Solids and Structures Under Moving Loads”, Noordhoff International Publishing, Groningen, The Netherlands, 1972.

- [3] Danish Roads Directorate (DRD) Report 291, “Reliability-Based Classification of the Load Carrying Capacity of Existing Bridges”, Roads Directorate, Ministry of Transport, Denmark, 2004.
- [4] E.J. OBrien, A. González, J. Dowling, A. Žnidarič, “Direct measurement of dynamics in road bridges using a bridge weigh-in-motion system”, *The Baltic Journal of Road and Bridge Engineering*, 11(4), 263-270, 2013.
- [5] D. Cantero, E.J. O'Brien, R. Karoumi, "Extending the Assessment Dynamic Ratio to Railway Bridges", in "Proceedings of the Second International Conference on Railway Technology: Research, Development and Maintenance", J. Pombo, (Editor). Civil-Comp Press, Stirlingshire, UK, Paper 67, 2014.
- [6] T. W. Parks and C. S. Burrus, “Digital Filter Design”, John Wiley & Sons, Texas, United States, 1987.
- [7] L.R. Rabiner, J.H. McClellan, T.W. Parks, “FIR Digital Filter Design Techniques Using Weighted Chebyshev Approximation”, in “Proceedings of the IEEE” 63, 595-610, 1975.
- [8] BD 37/01 “Loads for Highway Bridges”, in Design Manual for Roads and Bridges, Volume 1, Section 3, Part 14, Highways Agency, UK.
- [9] BD 21/01 “The Assessment of Highway Bridges and Structures”, in Design Manual for Roads and Bridges, Volume 3, Section 4, Part 3, Highways Agency, UK.
- [10] L. Connolly, A. O'Connor & E.J. Obrien, “Probabilistic modelling and assessment of railway bridges”, in “8th International Conference on Bridge Maintenance, Safety and Management” (2016 – in press).
- [11] Midas Information Technology Co., Ltd. Midas Civil Available at: http://en.midasuser.com/product/civil_overview.asp [Accessed 10 August 2015]
- [12] E. Castillo, “Extreme Value Theory in Engineering”, Academic Press Inc., London, United Kingdom, 1988.
- [13] ISO 2394, “General Principles on Reliability for Structures”, 1998.
- [14] JCSS, Joint Committee of Structural Safety, “Probabilistic Model Code I – Basis of Design”, 2000.
- [15] A. O'Connor, C. Pedersen, L. Gustavsson, I. Enevoldsen, “Probability based assessment and optimised maintenance planning for a large riveted truss railway bridge”, *Structural Engineering International*. 19(4), 375 – 383, 2009.
- [16] EN 1991-2, 2003, “Eurocode 1: Actions on structures – Part 2: Traffic loads on bridges”, European Standard, CEN, Brussels, 2003.
- [17] E. J. OBrien, A. Bordallo-Ruiz, B. Enright, “Lifetime maximum load effects on short-span bridges subject to growing traffic volumes”, *Structural Safety*, 50, 113–122, 2014.